ASIAN JOURNAL OF PHARMACEUTICAL AND CLINICAL RESEARCH

INNOVARE ACADEMIC SCIENCES
Knowledge to Innovation

Vol 18, Issue 11, 2025

Online - 2455-3891
Print - 0974-2441

Research Article

FORMULATION OPTIMIZATION OF FENUGREEK EXTRACT LOADED NANO-STRUCTURED LIPID-DRUG-CARRIER FOR EFFECTIVE ORAL DELIVERY

ADITI AGRAWAL, PRAKASH K SONI*, REENA SONI, SURESH K PASWAN

Nanotechnology Research Lab, Department of Pharmacy, Shri G. S. Institute of Technology and Science, Indore, Madhya Pradesh, India.
***Corresponding author:** Prakash K Soni; Email: soniprakashpharma@gmail.com

Received: 13 August 2025, Revised and Accepted: 08 October 2025

ABSTRACT

Objectives: The present work focused on designing, optimizing, and evaluating solid lipid nanoparticles (SLNs) for the oral delivery of fenugreek extract (FE) to achieve enhanced systemic bioavailability, higher gastrointestinal absorption, and sustained release kinetics.

Methods: A Box-Behnken statistical design was implemented to optimize FE-SLNs formulation by systematically varying lipid (compritol 888 ATO), surfactant (polyvinyl alcohol), and homogenization speed as processing parameter. Critical quality attributes including mean particle size, polydispersity index (PDI), surface charge (zeta potential), encapsulation efficiency (%EE), and release behavior (% cumulative drug release [CDR]) were analyzed. The final formulation was further characterized by advanced analytical techniques (transmission electron microscopy, differential scanning calorimeter) and evaluated for *ex vivo* intestinal permeation.

Results: The optimized FE-SLNs demonstrated favorable characteristics, average diameter (460 nm), uniform distribution (PDI 0.233), surface charge (−14.1 mV), and %EE (47.56%). *In vitro* studies showed %CDR (79.66% over 12 h). Permeation assessments revealed significantly enhanced absorption compared to FE solution, with permeability coefficients increasing from 2.9×10^{-3} cm/h (FE solution) to 6.3×10^{-3} cm/h (developed formulation).

Conclusion: The developed FE-SLNs system exhibited optimal physicochemical properties and enhanced absorption potential, demonstrating its successful formulation. The sustained release profile following Higuchi kinetics suggested that these nanoparticles could serve as an effective platform for oral administration of natural bioactives.

Keywords: *Trigonella foenum-graecum*, Lipid nanoparticles, Bioavailability enhancement, Experimental design, Sustained release, Intestinal absorption.

 DOI: http://dx.doi.org/10.22159/ajpcr.2025v18i11.56511. Journal homepage: https://innovareacademics.in/journals/index.php/ajpcr

INTRODUCTION

Oral drug delivery is universally favored due to its non-invasive nature and can be taken easily. Consequently, oral route can be used for delivering both natural and synthetic compounds [1,2]. Oral route is hindered by the challenging environment and physiological barriers within the gastrointestinal (GI) tract including its anatomy and physiology [3]. Medications administered orally can be absorbed through four main pathways: Transcellular (across cells), paracellular (between cells), carrier-mediated (transport proteins), and facilitated transport (assisted diffusion), with transcellular transport being the primary mechanism [2,4,5]. A critical consideration in oral drug formulation is bioavailability, which refers to the fraction of the administered dose that reaches systemic circulation intact [6].

Natural bioactives or phytoconstituents are known to treat the root cause of various diseases without adverse effects. Different widely used natural compounds exhibit properties such as antioxidant, antiallergic, anticarcinogenic, immunomodulatory activities [7,8]. Diverse group of bioactive compounds includes flavonoids, phenolic acids and tannins, alkaloids, terpenoids, carotenoids, fatty acids, etc. Despite today's advanced pharmaceuticals, traditional herbal medicines remain widely used due to their therapeutic effects and health-boosting nutrients continue to make them valuable for prevention and treatment [9-14].

Plant-based therapies are hindered by poor solubility, limited stability, and the complexity of isolating active compounds. Their multiple phytochemicals can cause formulation instability, while only a small fraction of the active component typically reaches the target site. Achieving precise, site-specific delivery therefore remains a major challenge [14,15].

Trigonella foenum-graecum L., commonly called as fenugreek, which is known to be one of the world's most ancient medicinal herbs [16]. Similarly, the extract of fenugreek have several health benefits such as anti-inflammatory activity, antidiabetic effect, antioxidant activity, and also used for cardiovascular diseases, hormone regulation, obesity, and GI related problems [17,18]. Phytochemical studies of fenugreek have shown that it contains many types of secondary compounds, includes saponins, steroids, alkaloids, flavonoids, terpenes, phenolic acid derivatives, amino compounds, and fatty acids. These bioactive fiber components exhibit significant nutraceutical potential for metabolic regulation [19]. Although a variety of traditional dosage forms are available in the market, they often exhibit significant limitations, including the poor solubility and permeability of flavonoids, saponins and alkaloids, as well as their instability in the GI environment, poor dissolution, low absorption, and extensive first pass metabolism. These drawbacks contribute to reduced bioavailability and suboptimal therapeutic outcomes [20]. These challenges necessitate a delivery system capable of enhancing solubility, protecting labile compounds, and improving intestinal uptake.

Nanomedicines and nano-systems have appeared as promising strategy, particularly for oral administration [21-23]. Nanocarriers offer multiple advantages, such as protection of medicament from degradation in harsh GI environment, enhanced absorption, site-specific targeting, and controlled or sustained drug release [24].

For these problems, solid lipid nanoparticles (SLNs) offer a promising strategy by encapsulating drug molecule within a lipid matrix to improve solubilization, confer protection against degradation, and facilitate controlled release and absorption. Typically, inert and biodegradable lipidic components make up solid core of nanocarrier, which carries both hydrophilic as well as hydrophobic drugs and are stabilized by emulsifying layer in an aqueous dispersion [25-27]. These systems offer several benefits like enhanced medicaments solubility and dissolution, improved stability, prolonged systemic circulation and targeted delivery with reduced adverse effects [28,29]. The incorporation of medicament into SLNs can occur through different models [30,31]. An important benefit of SLNs is that, they are absorbed by the body's reticuloendothelial system and can avoid being broken down during the first-pass effect [32]. Consequently, there is a need to develop delivery systems that can stabilize these bioactive compounds and enhance their bioavailability [33]. For oral formulation, such systems typically require three key components: lipid, a surfactant, and water [27,34].

Hence, by encapsulating fenugreek extract (FE) in SLNs will enhance the oral bioavailability of its poorly soluble and permeable bioactives through improved solubility, stability, and intestinal permeability.

This study focused to formulate and optimize FE-SLNs, to characterize their physicochemical and release properties, and to evaluate *ex vivo* intestinal permeability. The FE-SLNs were prepared using compritol 888 ATO (lipid) and polyvinyl alcohol (PVA) (surfactant) through high-speed homogenization and probe sonication. For optimization a Box-Behnken design (BBD) was utilized with lipid concentration, surfactant amount and homogenization speed as key factors. The responses measured were particle size, polydispersity index (PDI), surface charge, % encapsulation efficiency (EE), and drug release over time. The optimized FE-SLNs were thoroughly tested for physical and chemical properties (size, charge, and uniformity) drug release behavior (kinetics and duration), permeability (*ex vivo* studies to check absorption), shape and structure (Transmission Electron Microscopy [TEM] imaging), thermal properties differential scanning calorimeter (DSC) analysis.

MATERIALS AND METHODS

Materials

FE was supplied as a research sample by Arjuna naturals Pvt. Ltd. (India). Compritol 888 ATO was obtained from Gattefosse (Mumbai, India), while PVA and dialysis membrane-110 was procured from Himedia Laboratories Pvt. Ltd. (India) and chloroform from Merck (India). All the required excipients and solvent were of laboratory-grade quality. Milli-Q water (Ultrapure Type-1) was utilized for all procedures.

Preparation of FE-loaded SLNs

FE-loaded SLNs were developed through high-speed homogenization and further sonication was used for size reduction, as illustrated in Fig. 1. The SLNs were comprised of a lipid (compritol 888 ATO) and a surfactant (PVA). For organic phase, the lipid was dissolved in chloroform (5 mL) using a vortex mixer. FE and PVA were dissolved in warm milli-q water (50 mL) to obtain aqueous phase. Both the phases were heated to a temperature of 80–85°C, higher than melting point of lipid to ensure uniformity.

Further, organic phase was slowly injected in aqueous phase with continuous homogenization using a high-shear homogenizer (Polytron PT 3100, Kinematica) for 10 min. The resultant dispersion was mechanically stirred at 1000 rpm for 1 h at 60°C for removal for organic solvent and to enhance homogeneity. To achieve small particle size, the homogenized dispersion was ultrasonicated (Sonics VCX 500) for 5 min using a 3 mm tapered microtip at 30% amplitude. This process facilitated the transformation of coarse dispersions into finer nanoparticles. The final formulation was through microscope (Leica DM1000) to assess particle morphology [35].

DoE optimization of FE-loaded SLNs

Experimental design

The formulation optimization of FE-SLNs was conducted using Design Expert software (Version 12, Stat-Ease Inc., Minneapolis, MN, USA), employing a three-factor, three-level, BBD [36,37]. Three critical formulation parameters were selected as independent variables, lipid content (compritol 888 ATO, denoted as F1), surfactant concentration

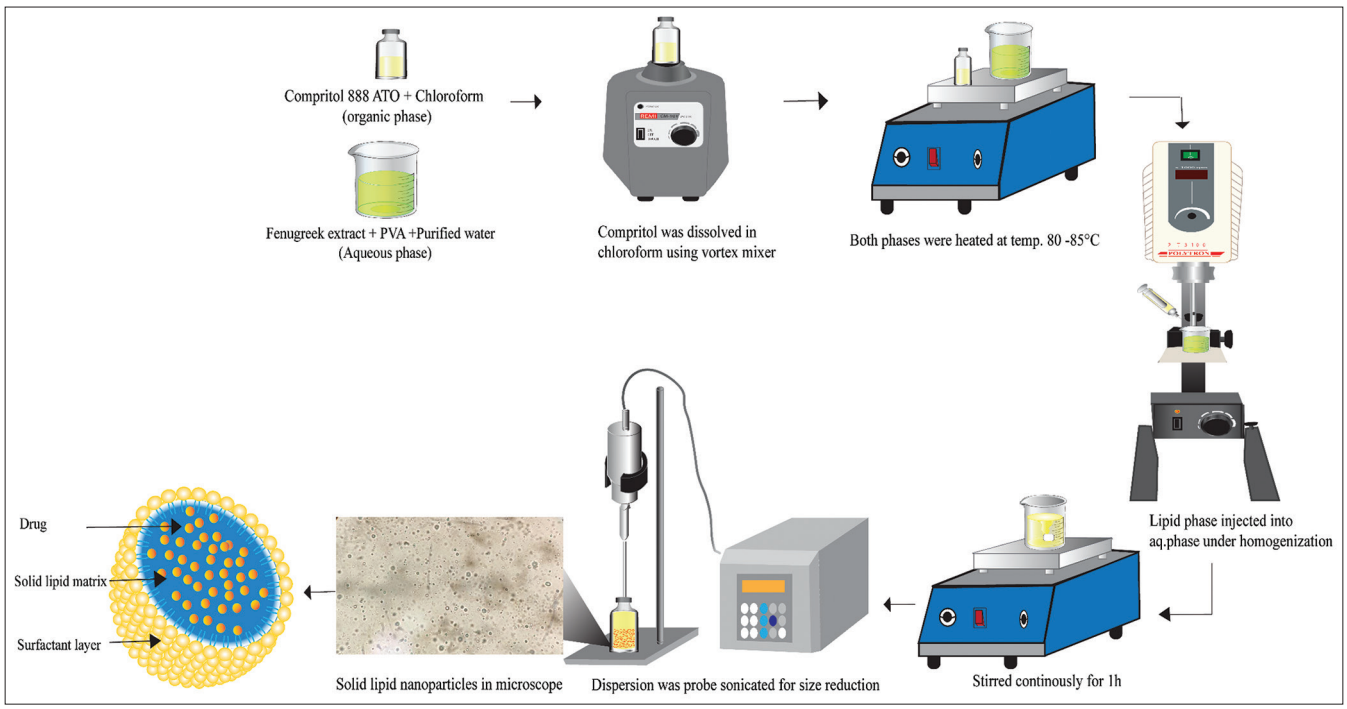

Fig. 1: Diagrammatic presentation of development of fenugreek extract incorporated solid lipid nanoparticles

(PVA, denoted as F2), and homogenization speed (rpm, denoted as F3), and each was evaluated at three coded levels (−1, 0, +1) low, medium, and high values, respectively. The response variables includes critical quality attributes (CQAs), i.e., mean particle size (MPS), zeta potential (ZP), PDI, % EE, % cumulative drug release (CDR) at 0.5, 1, 4, 8 and 12 h and were denoted as R1-R9, respectively and are shown in Table 1. The software generated experimental design comprised 15 randomized runs (SLN1–SLN15), with the variable combinations and corresponding responses detailed in Table 2.

Statistical analysis

Fifteen optimization batches of FE-SLNs (SLN1–SLN15) were formulated and characterized for response variables (R1 to R9) as shown in Table 2. The findings were then inserted into design expert software for statistically fitting into linear, 2FI, quadratic, and cubic models. The fitting process considered metrics such as predicted R^2, adjusted R^2, lack of fit p-values, and sequential p-values. Based on statistical validation through ANOVA, the software identified the most suitable model for each response parameter. Specifically, a linear model was found to best describe the data for MPS, PDI, %EE and %CDR (1, 4 and 12 h). Meanwhile, a quadratic model provided the best fit for ZP, and %CDR (0.5and 8 h). The significance of model was confirmed with $p<0.05$, as summarized in Table 3.

Response surface analysis and optimization standards

Three-dimensional (3D) response surface plots were generated for each response to evaluate the impact of formulation factors on corresponding responses, as shown in Figs. 5-13. For selection of the ideal formulation composition for FE-SLNs, the optimized independent variables were target as, lipid (compritol 888 ATO) in range (F1), surfactant (PVA) in range (F2), and homogenization speed in range (F3) while the dependent variables were set as minimum MPS and PDI, maximum ZP, %EE, and %CDR for FE-SLN (0.5, 1, 4, 8 and 12 h). Optimization goals mentioned in Table 1 for input variables and output response were set in software and suggested an optimized component with highest desirability in the response.

Table 1: Process variables and response parameters for optimization of FE-SLNs

Process variable	Unit	Levels		
		Low	Medium	High
F1: Compritol 888 ATO	mg	400	500	600
F2: PVA	%	0.2	0.35	0.5
F3: Homogenization speed	rpm	10,000	12,500	15,000
Response parameters	**Target specification**			
R1: Particle Size (nm)	Minimum			
R2: Zeta potential (mV)	Maximum			
R3: PDI	Minimum			
R4: Entrapment efficiency (%)	Maximum			
R5: Cumulative % drug release at 0.5 h	Maximum			
R6: Cumulative % drug release at 1 h	Maximum			
R7: Cumulative % drug release at 4 h	Maximum			
R8: Cumulative % drug release at 8 h	Maximum			
R9: Cumulative % drug release at 12 h	Maximum			

Characterization of FE-loaded SLNs

Particle size determination, PDI and ZP

The MPS, PDI, and surface charge of all the prepared formulation were analyzed using Nanotrac wave II (Microtrac) particle size analyzer [38,39]. The principle involved in ZP analysis was laser Doppler electrophoresis technique and dynamic light scattering in MPS and PDI. All the observations are shown in Table 2.

Determination of EE

EE of FE-SLNs was estimated using centrifugation method, as represented in Fig. 2. About 2 mL of SLN formulation of FE was taken in Eppendorf tube and centrifuged at 10,000 rpm for 15 min through high-speed cooling centrifuge (C-24 Eppendorf). After centrifugation, SLNs were then lysed by chloroform: water (1:9), this mixture was bath sonicated for 5 min and kept undisturbed overnight. Then filtered out and analyzed through ultraviolet (UV)-visible spectrophotometer (Shimadzu 1700) at 273 nm. The %EE was estimated by given formula:

$$\text{Entrapment efficiency}(\%w/w) = \frac{\text{Total amount of drug entrapped}}{\text{Total amount of drug added}} \times 100$$

In vitro drug release

For determination of FE release from FE-SLNs (SLN1-SLN15), dialysis membrane method was implemented [40,41]. For these, dialysis membrane (Dialysis Membrane-110, Himedia, India) was taken and activated as previously reported [1,42,43].

Each membrane was cut into 5 cm length and sealed from one end [44]. Then, sufficient volume SLN formulation was carefully placed into dialysis pouch and other end was also closed using a closure clip. The bags were placed into PBS (pH 6.8) and agitated at 100 rpm, maintained at body temperature as illustrated in Fig. 3. At specified time points (0.5, 1, 4, 8 and 12 h), samples were collected and replenished with equal volume of fresh buffer.

The withdrawn samples were analyzed by UV-Vis spectrophotometer (Shimadzu 1700) at 273 nm and % CDR for FE at various time intervals was calculated and data are tabulated in Table 2 and illustrated graphically in Fig. 14.

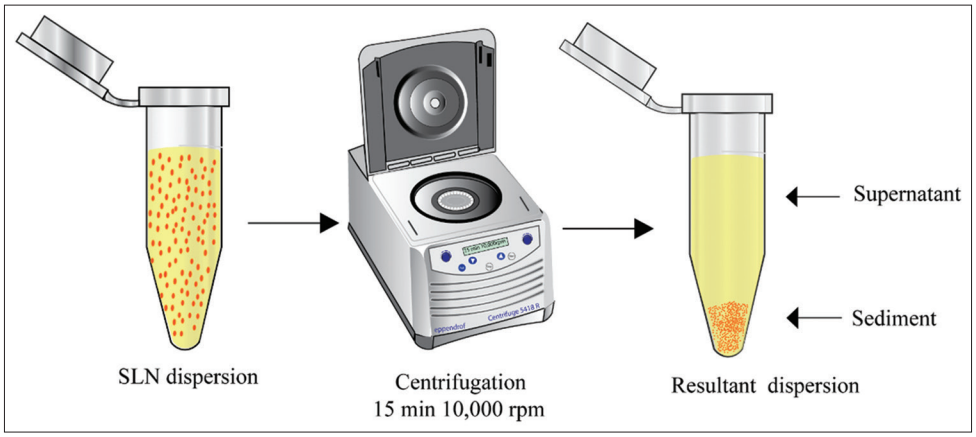

Fig. 2: Schematic representation of separation and filtration of FE-SLNs via centrifugation

Table 2: Observation of responses of the optimization (SLN1-SLN15) batches

S. No.	Independent variables			Response variables							
Batch No.	F1: A: lipid content (mg)	F2: B: surfactant conc. (%)	F3: C: homogenization speed (rpm)	R1: MPS (nm)	R2: ZP (mv)	R3: PDI	R4: EE (%)	R5: %CDR at 0.5 h (%)	R6: %CDR at 1 h (%)	R7: %CDR at 4 h (%)	R8: %CDR at 8 h (%)	R9: %CDR at 12 h (%)
SLN 1	500	0.5	10000	620	−11.8	0.227	49.12	14.45±1.48	20.62±2.92	39.71±5.21	60.41±2.79	84.64±3.17
SLN 2	600	0.35	10000	896	−9.4	0.298	63.92	10.46±2.74	17.22±3.09	32.33±3.46	55.88±3.17	70.23±2.88
SLN 3	400	0.5	12500	384	−17.1	0.349	38.32	19.7±4.59	23.00±2.87	48.44±4.18	70.50±1.75	88.5±5.40
SLN 4	500	0.2	15000	728	−2	0.855	61.92	12.96±2.23	18.27±1.98	35.88±3.62	54.7±3.56	73.67±5.20
SLN 5	600	0.2	12500	928	−7.2	0.724	65.12	8.90±1.08	16.75±3.11	30.92±4.65	51.95±1.04	68.49±2.90
SLN 6	500	0.35	12500	679	18.7	0.369	59.92	13.72±2.14	18.68±1.39	37.17±2.08	58.9±2.09	72.57±3.28
SLN 7	600	0.5	12500	856	8	0.363	40.52	13.22±2.05	20.5±2.72	36.76±3.79	60.21±2.70	78.24±5.35
SLN 8	400	0.2	12500	478	8.3	0.577	52.32	16.56±2.88	20.48±3.01	35.2±5.03	59.34±3.02	83.35±4.16
SLN 9	500	0.35	12500	725	18	0.336	57.12	13.29±4.30	20.97±1.23	34.16±3.77	60.39±4.47	80.39±1.63
SLN 10	500	0.2	10000	735	4.4	0.59	62.72	10.83±1.54	20.34±6.92	33.64±1.62	50.86±4.25	74.33±1.01
SLN 11	500	0.5	15000	460	−10.4	0.223	48.72	15.72±1.84	21.55±4.29	41.37±3.63	61.21±1.62	79.62±3.61
SLN 12	400	0.35	10000	445	−9.3	0.147	42.32	17.73±2.29	19.76±2.99	42.11±3.15	68.16±2.01	82.22±2.91
SLN 13	400	0.35	15000	413	−15.2	0.441	45.12	18.43±4.71	22.45±4.60	46.25±5.81	64.18±2.06	85.03±4.38
SLN 14	500	0.35	12500	730	8.9	0.783	57.52	13.25±2.74	22.1±3.26	37.04±5.34	57.83±3.39	70.25±1.85
SLN 15	600	0.35	15000	879	−7.6	0.783	67.52	12.86±2.33	15.26±2.64	34.22±2.84	58.79±3.17	65.78±3.97

Development of optimized formulation (final batch) of FE-SLNs

The final batch of FE-SLNs, as proposed by the Design expert software, consists of 400 mg (compritol 888 ATO), 0.303% (PVA) and 12610.6 rpm (homogenization speed) achieving maximum desirability value 0.658 was formulated by utilizing high-speed homogenization and sonication method. The highest desirability of optimized composition is represented in 2D contour and 3D response surface plots as presented in Fig. 15. The optimized FE-SLNs formulation was developed and experimentally evaluated to perform the validation of software prediction. To test the predicted optimal batch, FE-SLNs were prepared using the suggested composition and all response variables were thoroughly characterized to compare the experimentally obtained values with the software-predicted theoretical values for each quality attribute and their results are tabulated in Table 4. A comparative release profiles were generated, where predicted and observed drug release kinetics were overlaid across all time points (Fig. 18a) and a linear regression plot was constructed between experimentally observed versus software predicted drug release data (Fig. 18b).

Assessment of final batch of FE-SLNs

TEM and Optical microscopic analysis

For the TEM analysis of optimized FE-SLNs batch, approximately 2–5 µL of sample was placed on the grid of TEM with the help of pipette and sample was dried about 2–3 min for proper adsorption. After this, the excess sample was removed for even distribution. Prepared sample was examined by TEM (Talos L120C G2, thermo fisher) UV at 120 KV voltage with magnification between 34X and 6,50,000X. TEM image of final batch of FE-SLNs is revealed in Fig. 16.

The microscopy of the final batch of FE-SLNs was performed using microscope (Leica DM 1000) with 100X oil immersion lens. The resulting image is presented in Fig. 16.

MPS (R1), ZP (R2), PDI (R3)

MPS, PDI, and ZP of the final batch of SLNs were analyzed using Nanotrac wave II particle size analyzer (Microtrac). The particle size distribution results are summarized in Table 4 and graphically represented in Fig. 17.

Entrapment efficiency (R4)

Drug EE was determined by centrifugation method as discussed in previous section and recorded data is shown in Table 4.

In vitro drug release and drug release kinetics

An experiment of drug release from FE-SLNs were processed through dialysis method, as mentioned earlier. The concentration of FE was analyzed by UV-visible spectrophotometer (Shimadzu 1700) at 273 nm. At multiple time points %CDR was calculated and tabulated in Table 4. Kinetic modeling of the FE-loaded SLN's drug release data was performed using zero-order, first-order, Korsmeyer-Peppas, Higuchi, and Hixson-Crowell equations as shown in Fig. 19 [45].

DSC study

The thermal analysis of lyophilized FE-SLNs, compritol 888 ATO, PVA, FE, and their physical mixture (compritol 888ATO+PVA+FE) was performed by DSC (Perkins Elmer 6000, Walthman, MA, USA). Each sample was weighed 3–5 mg and placed in aluminum pan and sealed [46]. These pans were positioned in the sample holder, with a blank aluminum pans used as reference [47]. The thermograms were generated by scanning the FE and excipients at rate of 40ºC/min between temp. 50°C and 300°C which shown in Fig. 20.

Ex vivo drug absorption study

This study utilized everted gut sac method to evaluate GI absorption of FE-SLNs and FE solution. A fresh lower GIT from a healthy chicken was obtained from a local slaughterhouse. The ileum segment was carefully isolated, thoroughly washed, and cut into 6 cm length [48].

Table 3: Measured response variables obtained using fit summary by Box-Behnken design

Response variables	Source	Sequential p-value	Lack of Fit p-value	Adjusted R^2	Predicted R^2	Remarks
R1: Particle size	Linear	< 0.0001	0.2519	0.9345	0.9067	Suggested
	2FI	0.5119	0.2263	0.9314	0.8623	-
	Quadratic	0.2601	0.2460	0.9475	0.7444	-
	Cubic	0.2460	-	0.9775	-	Aliased
R2: Zeta potential	Linear	0.7419	0.1465	-0.1418	-0.4548	-
	2FI	0.4753	0.1330	-0.1684	-0.5948	-
	Quadratic	0.0023	0.8293	0.8745	0.7096	Suggested
	Cubic	0.8293	-	0.7828	-	Aliased
R3: PDI	Linear	0.0023	0.9912	0.6429	0.5995	Suggested
	2FI	0.8008	0.9807	0.5638	0.5150	-
	Quadratic	0.8385	0.9446	0.4022	0.0930	-
	Cubic	0.9446	-	-0.2772	-	Aliased
R4: %EE	Linear	0.0012	0.0620	0.6816	0.5052	Suggested
	2FI	0.8561	0.0457	0.6003	-0.0438	-
	Quadratic	0.2311	0.0508	0.7102	-0.6075	-
	Cubic	0.0508	-	0.9753	-	Aliased
R5: %CDR at 0.5 h	Linear	< 0.0001	0.0745	0.9209	0.8800	-
	2FI	0.6932	0.0595	0.9084	0.7762	-
	Quadratic	0.0031	0.3755	0.9890	0.9516	Suggested
	Cubic	0.3755	-	0.9926	-	Aliased
R6: %CDR at 1 h	Linear	0.0089	0.7130	0.5378	0.3321	Suggested
	2FI	0.3522	0.7335	0.5681	0.1473	-
	Quadratic	0.3216	0.8172	0.6366	0.1331	-
	Cubic	0.8172	-	0.3842	-	Aliased
R7: %CDR at 4 h	Linear	< 0.0001	0.4184	0.8263	0.7459	Suggested
	2FI	0.4461	0.3977	0.8257	0.6301	-
	Quadratic	0.3576	0.3911	0.8460	0.3330	-
	Cubic	0.3911	-	0.8916	-	Aliased
R8: %CDR at 8 h	Linear	0.0004	0.1745	0.7443	0.5801	-
	2FI	0.5834	0.1494	0.7207	0.1934	-
	Quadratic	0.0141	0.5071	0.9376	0.7585	Suggested
	Cubic	0.5071	-	0.9413	-	Aliased
R9: %CDR at 12 h	Linear	0.0006	0.8921	0.7252	0.6549	Suggested
	2FI	0.6865	0.8468	0.6828	0.5283	-
	Quadratic	0.3167	0.9637	0.7349	0.6442	-
	Cubic	0.9637	-	0.4100	-	Aliased

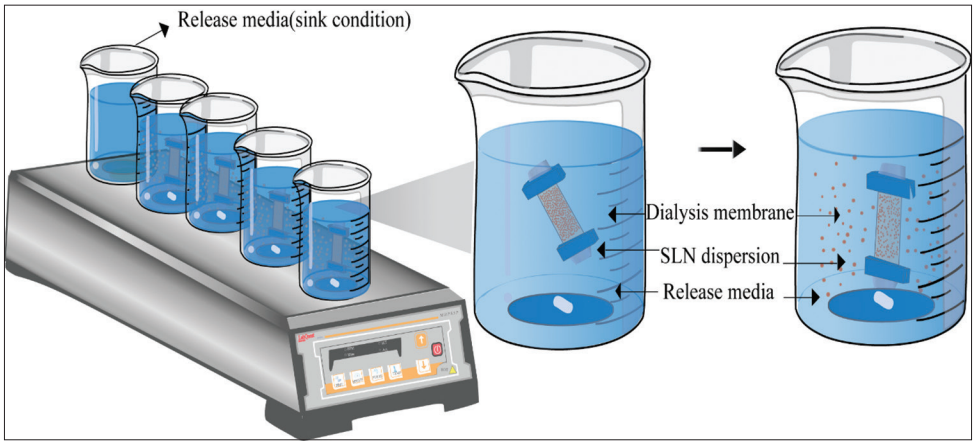

Fig. 3: Diagrammatic illustration of *in vitro* drug release method of FE loaded SLNs using dialysis bag method

These segments were then washed out with PBS (pH 6.8) Each piece was gently slipped onto a glass rod, tied at one end with thread, and carefully everted [1,49]. A drug solution containing 2 mg/mL of FE, (equivalent to the main formulation) was prepared for study. 1 mL of each, developed formulation and the FE solution was filled into individual everted sacs and tied using a thread from the other end. These segments were submerged in 100 mL of PBS (pH 6.8), with human body temp at medium stirring to mimic intestinal conditions and facilitate drug permeation across the intestinal membrane. The samples were taken out (0.5 1, 4, 8 and 12 h) and buffer was used to uphold sink conditions. Assembly of *ex vivo* absorption study is depicted in Fig. 4.

The amount of FE that permeated over a set period of time was estimated at 273 nm by UV-Visible spectrophotometer (Shimadzu 1700).% drug permeated was calculated and the data is summarized in Table 5 and graphically represented in Fig. 21. The apparent permeability coefficient (P_{app}) and steady-state drug permeation flux (J_{ss}) of FE in prepared solution and the optimized batch, was determined using equation.

$$P_{app} = (dQ/dt)/(C0*A)$$

$$J_{ss}=P_{app}*C$$

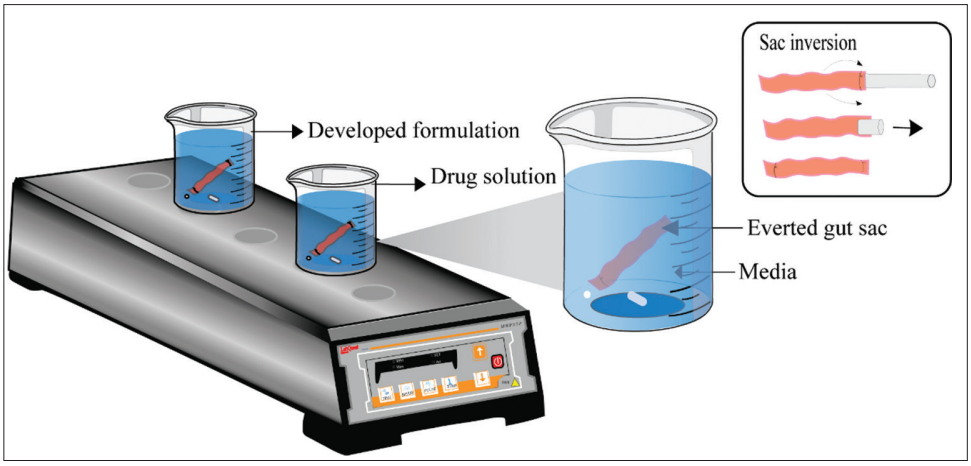

Fig. 4: Schematic presentation of ex vivo drug absorption study

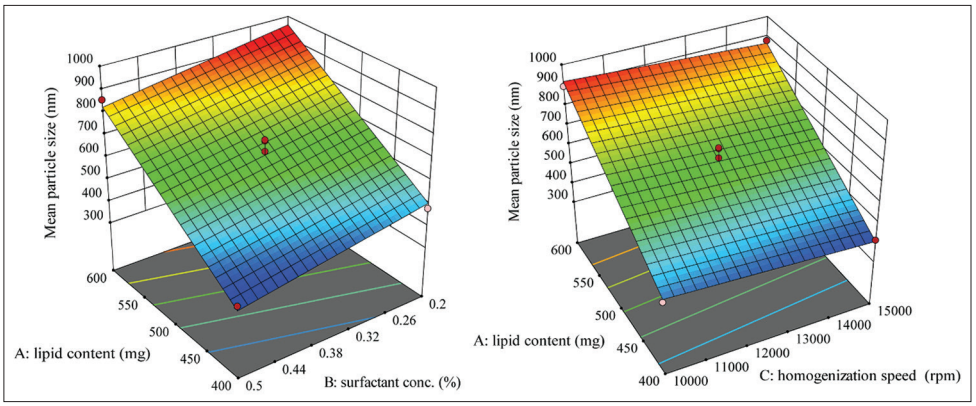

Fig. 5: 3D plots depicting effect of lipid, surfactant and homogenization speed on mean particle size

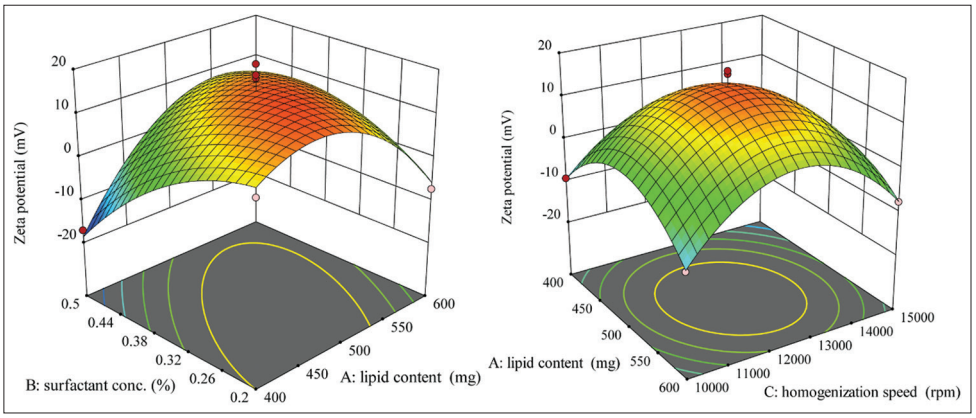

Fig. 6: 3D plots depicting effect of lipid, surfactant and homogenization speed on zeta potential

In this context, permeability rate is represented by dQ/dt, A stands for area of the intestinal section, and C_0 represents primary conc.

RESULTS AND DISCUSSION

Preparation of FE-loaded SLNs

We designed FE-loaded SLNs using compritol 888 ATO and PVA for oral delivery of FE to overcome its biopharmaceutical limitations. Biocompatibility, biodegradability, and versatility served as the primary criteria for component selection. Compritol consists of glycerol with behenic acid esters, while PVA is used as a stabilizer in lipid nanoparticles to enhance their colloidal stability and prevent aggregation. PVA acts as a non-ionic stabilizer, providing stereo static stabilization to the nanoparticles which helps in creating a stable dispersion of lipid nanoparticles.

Optimization of FE-loaded SLNs

To achieve optimal quality attributes in FE-loaded SLNs, a Box-Behnken experimental design was implemented. This systematic approach facilitated optimization of key formulation parameters to attain desired CQAs, with minimized MPS and PDI for uniformity and stability, maximized ZP to enhance colloidal stability, improved %EE for effective drug loading and enhanced %CDR for optimal delivery. The influence of formulation factors on each response were assessed using response surface methodology (RSM), allowing for the identification of significant interactions and optimal processing conditions.

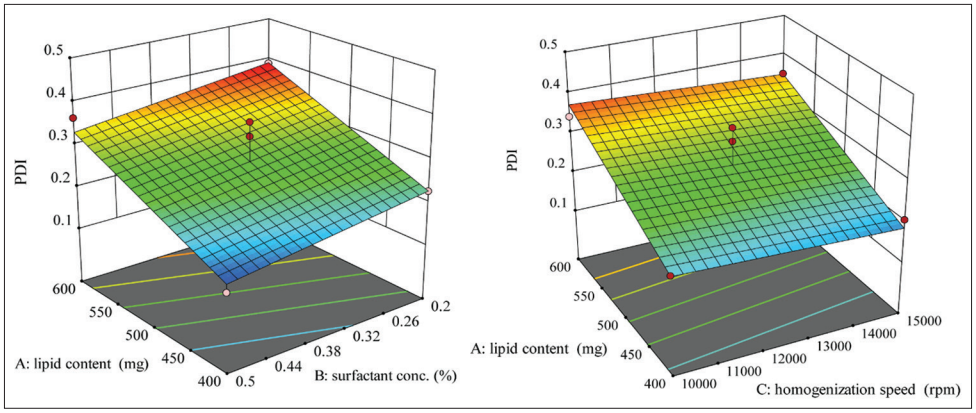

Fig. 7: 3D plots depicting effect of lipid, surfactant and homogenization speed on PDI

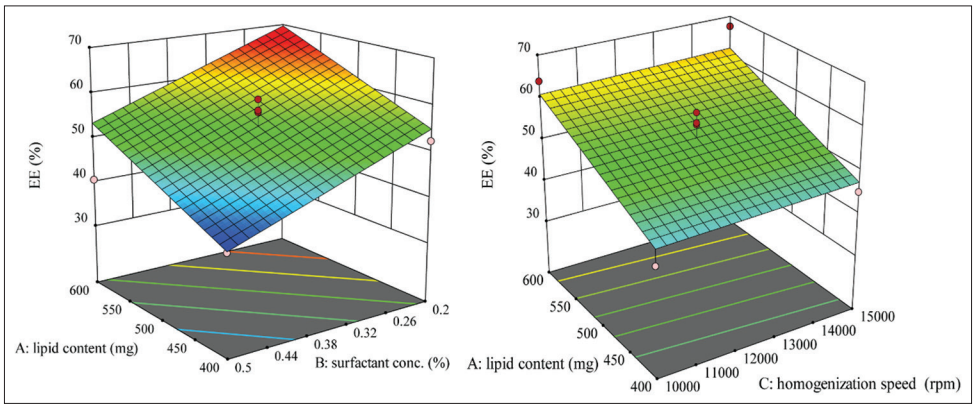

Fig. 8: 3D plots depicting effect of lipid, surfactant and homogenization speed on %EE

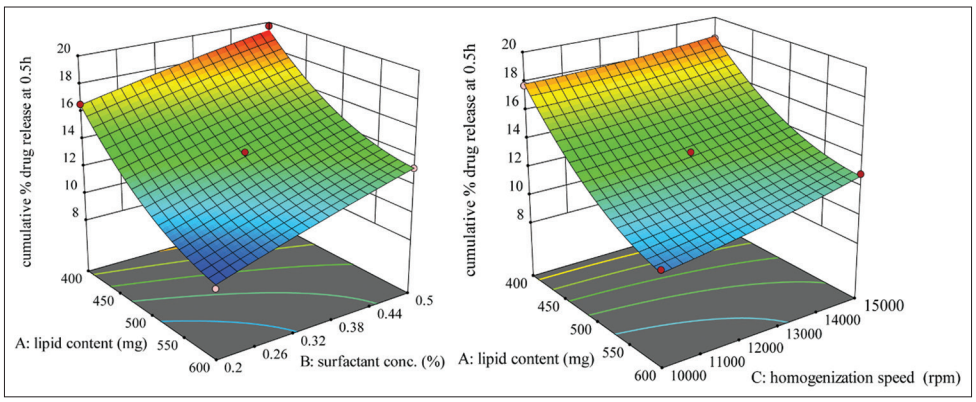

Fig. 9: 3D plots depicting effect of lipid, surfactant and homogenization speed on %CDR at 0.5 h

Table 4: Software predicted data and experimentally observed data of optimized formulation

Optimization formulation composition		**Measured Responses**		
Component	**Amount**	**Evaluation parameter**	**Software predicted value**	**Experimentally observed value***
F1: Lipid content	400 mg	Mean particle size (nm)	454.70	460.0±6.24
F2: Surfactant Conc.	0.303%	Zeta potential (mV)	5.526	−14.1±5.56
F3: Homogenization speed	12610.6 rpm	PDI	0.205	0.233±0.07
		EE (%)	49.36	47.56±4.11
		%CDRat 0.5 h	17.63	20.27±6.16
		%CDRat 1 h	21.46	22.06±1.85
		%CDRat 4 h	41.63	39.30±6.31
		%CDR at 8 h	64.83	57.52±5.89
		%CDR at 12 h	82.955	79.66±6.22

*Data presented as Mean±SD, (n=3)

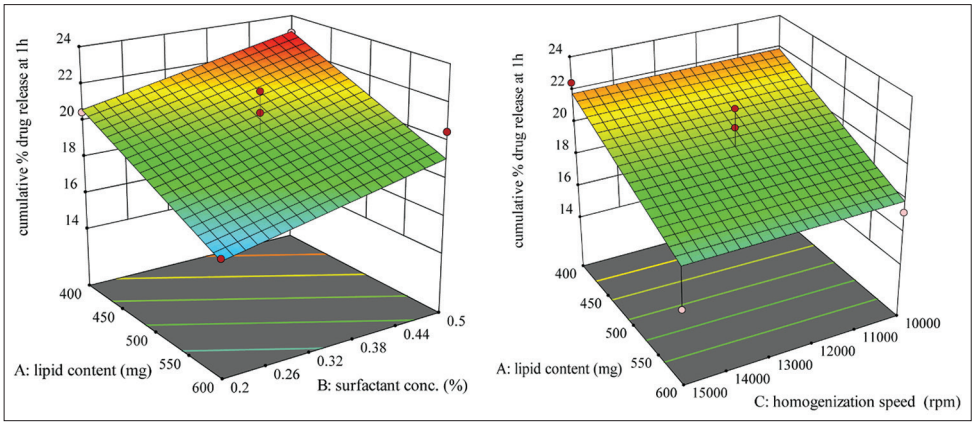

Fig. 10: 3D plots depicting effect of lipid, surfactant and homogenization speed on %CDR at 1 h

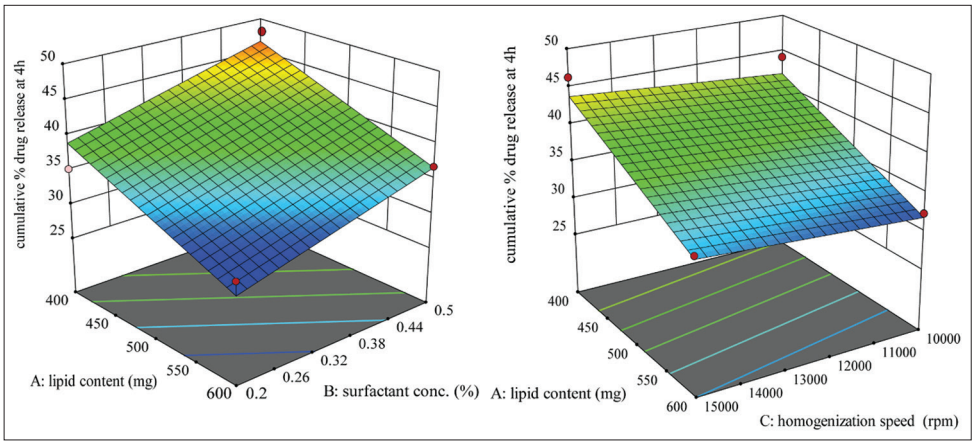

Fig. 11:3D plots depicting effect of lipid, surfactant and homogenization speed on %CDR at 4 h

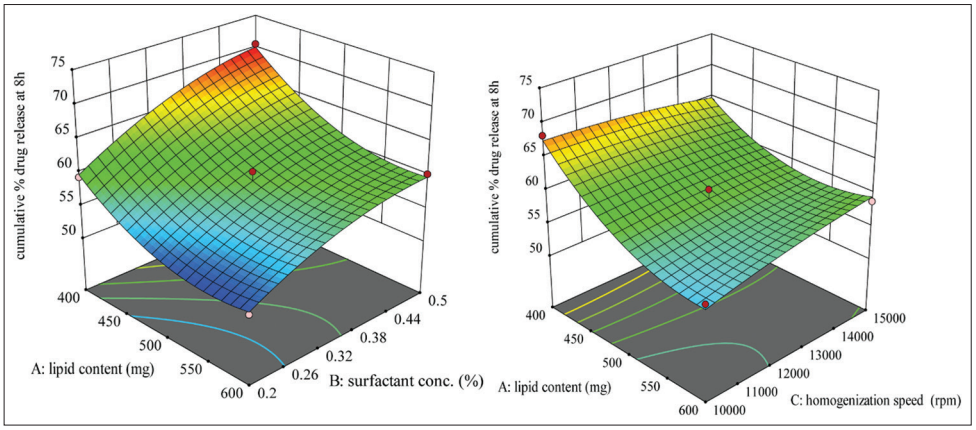

Fig. 12: 3D plots depicting effect of lipid, surfactant and homogenization speed on %CDR at 8 h

Relationship between formulation variables MPS

The impact of formulation factors on MPS (R1) was analyzed through RSMin Design Expert software. A linear model was fitted, demonstrating a direct relationship between the variables and particle size.

$$R1 = 663.73 + 229.87A - 68.63B - 27.00C$$

In the experiment, A is solid lipid (compritol 888 ATO), B is surfactant (PVA) and C is homogenization speed. Positive value of these factors suggests their direct effect and negative value indicates their indirect effect onto the MPS in equation. The particle size ranged from 384 to 928 nm across all the batches (SLN1-SLN 15) (Table 2). The 3D contour (Fig. 5) represents that when solid lipid content (compritol 888 ATO) increased, the MPS of the FE-SLNs also increased but when surfactant (PVA) conc. and homogenization speed increased it leads to decrease in MPS.

An increase in lipid content leads to rise in the viscosity of the dispersion. At lower homogenization speeds, higher lipid content promotes particle aggregation, thereby contributing to an increase in size. Increase in lipid levels significantly increase's both viscosity and surface tension, which collectively result into larger particle sizes. As

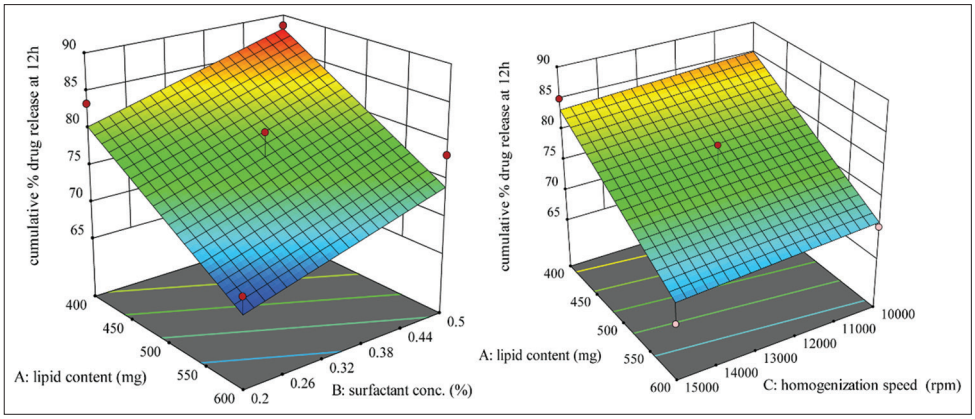

Fig. 13: 3D plots depicting effect of lipid, surfactant and homogenization speed on %CDR at 12 h

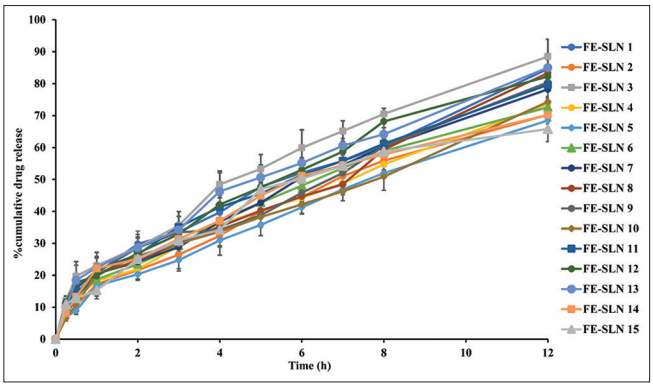

Fig. 14: Cumulative % drug release profile of optimization batches of fenugreek extract loaded FE-SLNs. Data plotted as mean±SD (n=3)

Table 5: Cumulative % drug permeation data of developed formulation and drug solution

Time (h)	Cumulative % drug permeated (FE)*	
	Developed formulation	Drug solution
0.5	33.51±1.87	13.20±2.65
1	39.09±2.02	15.42±3.02
4	54.09±3.08	24.12±2.61
8	83.75±3.12	36.80±2.06
12	90.90±2.69	40.58±3.17

*Data presented as Mean±SD, (n=3)

the content of solid lipid increases, particle size tends to rise due to vesicle accumulation and subsequent aggregation. Lowering in particle size was observed with increasing homogenization speed. This was attributed to the intensified shear forces generated at higher speeds, which facilitate the breakdown of emulsion droplets and consequently reduce particle size.

Relationship between formulation variables and ZP

Through RSM, Design Expert software established a quadratic relationship between the formulation variables and ZP (R2).

$$R2 = 15.2 + 2.1375A - 4.35B - 1.1375C + 10.15AB + 1.925AC + 1.95BC 11.3125A^2 - 5.887B^2 - 14.262C^2$$

The ZP for batches (SLN1–SLN15) ranged from −17.1 mV to 18.7 mV (Table 2). 3D plot (Fig. 6) portray that increment in lipid content (compritol 888 ATO) led to rise in ZP whereas, decreases in Z-potential was observed with increment in surfactant conc. and homogenization speed but optimum value showed high value of surface charge.

As the lipid content increases, ZP also elevates and it also raises the hydrophobic character of particles, leading to altered surface charge distribution and a slight increase in ZP (less negative/more positive) whereas, PVA is a non-ionic surfactant that adsorbs onto particle surfaces and forms a steric stabilizing layer or barrier, this barrier keeps the particles separated and prevents aggregation, even though electrostatic repulsion is weak. At higher concentrations, it may mask charge effects, leading to decline in ZP and higher homogenization speeds reduce particle size but also affect surface charge. Increased shear forces break aggregates, exposing new surfaces. If the stabilizer (PVA) does not fully cover these surfaces, charge neutralization or redistribution may occur which reduces ZP.

Relationship between formulation variables and PDI

Through RSM, Design Expert software established a linear relationship between the formulation variables and PDI (R3).

$$R3 = 0.2784 + 0.082125\ A - 0.0305B - 0.011625C$$

The PDI of batches (SLN1-SLN15) was found to be in the range of 0.147–0.389 (Table 2). The 3D contour (Fig. 7) represents when lipid content (compritol 888 ATO) increased, increment in PDI values was observed whereas, decrease in the PDI values was observed on increasing the surfactant conc. and homogenization speed.

As the lipid content increases, it leads to wider particle distribution due to lipid aggregation and results into the increase in PDI while, PVA and higher shear forces break down larger aggregates, leading to more uniform particle size distribution preventing aggregation and improving uniformity and leads to decrease in PDI results into better stabilization and uniformity [50].

Relationship between formulation variables and %EE

The design expert software, based on RSM, generated a linear model to describe the relationship between the formulation factors and EE (R4).

$$R4 = 54.1467 + 7.375A - 8.175B + 0.65C$$

The %EE (FE) of batches (SLN1–SLN15) was found in the range of 38.32% to 63.92% (Table 2). The 3D contour (Fig. 5) represents when lipid content (compritol 888 ATO) and homogenization speed increased, %EE was increased whereas, on increasing surfactant conc., decrease in the %EE was observed.

% Entrapment efficiency was enhanced by increasing the lipid content because compritol forms lipid matrix and it promotes better drug entrapment due to its hydrophobic nature and film-forming

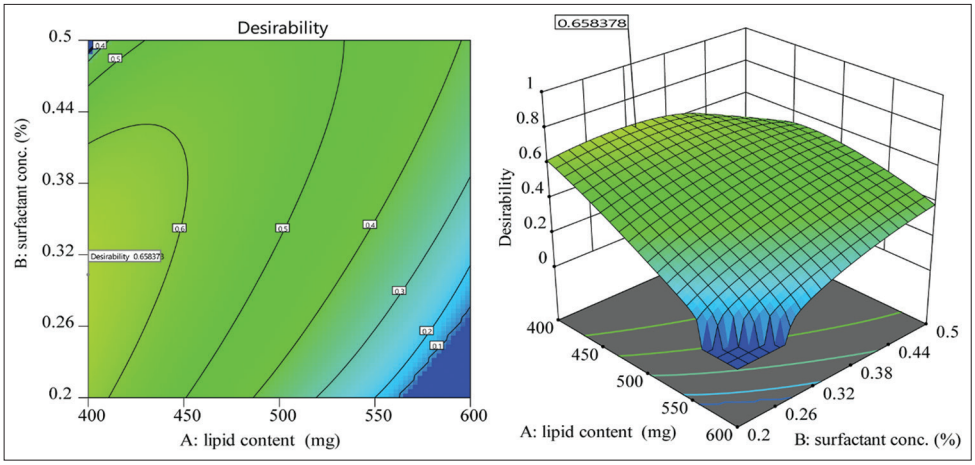

Fig. 15: 2D-contour and 3D-response surface plots showing highest desirability of optimized batch of FE-SLNs

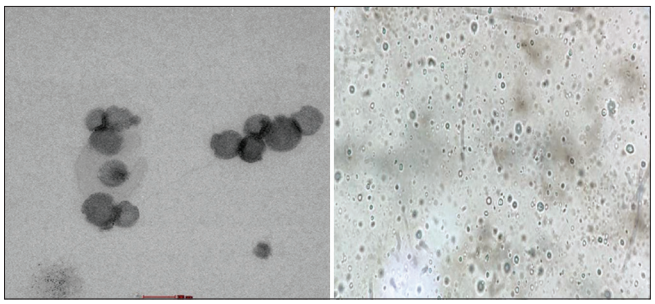

Fig. 16: Transmission electron microscopy and optical microscopic image of optimized fenugreek extract-solid lipid nanoparticles batch

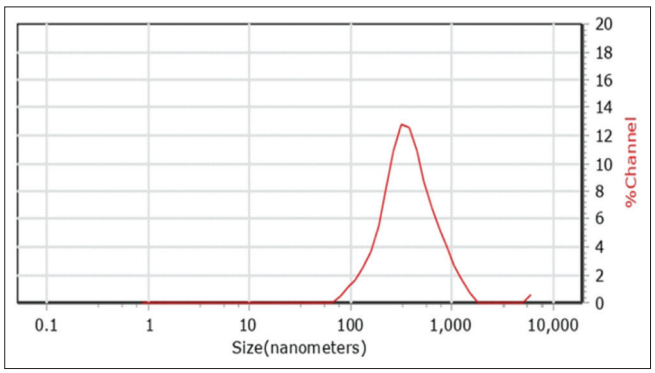

Fig. 17: Particle size distribution of optimized fenugreek extract-solid lipid nanoparticles

properties whereas, %EE was reduced at higher PVA conc. because it compete with the drug for interfacial space [51], leading to lower encapsulation and a marginal improvement in %EE was observed with increased homogenization speed because higher shear forces improve emulsification, leading to more uniform particle formation and slightly better drug retention.

Relationship between input variables and *in vitro* drug release

The design expert software using RSM expressed a relationship between input variables and %CDR at 0.5 h (R5), 1 h (R6), 4 h (R7), 8 h (R8) and 12 h (R9), by following process order equation:

$$R5 = 13.42 - 3.3725A + 1.73B + 0.8125C + 0.295AB + 0.425AC - 0.215BC + 1.2775A^2 - 0.1025B^2 + 0.1725C^2$$

$$R6 = 19.8635 - 1.99538A + 1.22912B - 0.05125C$$

$$R7 = 37.8133 - 4.97125A + 3.83B + 0.99125C$$

$$R8 = 59.04 - 4.41875A + 4.435B + 0.44625C - 0.725AB + 1.7225AC - 0.76BC + 3.20875A^2 - 1.74875B^2 - 0.49625C^2$$

$$R9 = 77.154 - 7.045A + 3.895B - 0.915C$$

%CDR of batches (SLN1–SLN15) was observed in between 8.9% and 19.7% at 0.5 h, 15.26% and 23.00% at 1 h, and 30.92% and 48.44% at 4 h, 50.86% and 70.5% at 8 h and 65.78% and 88.5% at 12 h (Table 2) and graphically represented in Fig. 14.

Three-dimensional contour (Figs. 9-13) represents when lipid content (compritol 888 ATO) increased, %CDR was decreased whereas, on increasing surfactant conc., increase in %CDR was observed, but no significant effect of homogenization speed was observed.

A consistent negative impact on drug release was observed with increasing lipid content, this was due to the formation of a more rigid and hydrophobic lipid matrix, which slows down drug diffusion [52] and PVA concentration consistently demonstrates a positive influence on drug release across all models. This enhancement was caused by the surfactant's ability to increase matrix hydrophilicity and create more porous structures. The negative value of (B^2) in R8 (−1.74875) showing that excessive PVA leading to saturation effects in release modification.

Optimized formulation of FE-loaded SLNs

The input variables included compritol 888 ATO (lipid, within a specified range), PVA (surfactant, within a range), and homogenization speed (within a range). The output responses were optimized for minimized MPS and PDI. Maximum ZP, % entrapment efficiency, and %CDR at predefined time points.

The software generated multiple solutions, from which the optimal batch with the highest desirability (0.658) was selected. The recommended formulation consisted of lipid (compritol 888 ATO, 400 mg), surfactant (PVA, 0.303% w/v), and homogenization speed (12,610.6 rpm).

The optimization was visualized using 3D-response surface plots and 2D-contour plots (Fig. 15). The optimized formulation was then prepared and evaluated, with experimental results aligning closely with the software's predictions (Table 4).

Evaluation of optimized formulation

Microscopic evaluation

These evaluation of the final batch of SLNs was performed and microscopic image (TEM and optical) depicted in Fig. 16 confirmed the spherical shape, uniformity with nano-sized SLNs which are desired for effective delivery.

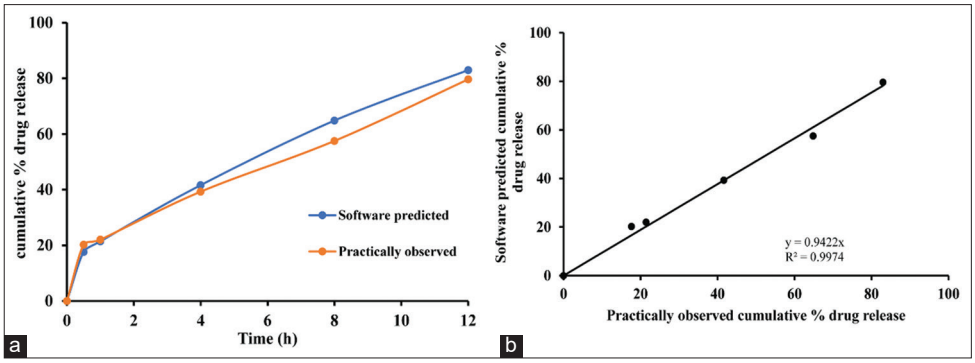

Fig. 18: (a) an overlay plot comparing the software predicted and experimentally measured cumulative % drug release profiles (b) Regression plot showing the correlation between predicted and observed cumulative % drug release profile

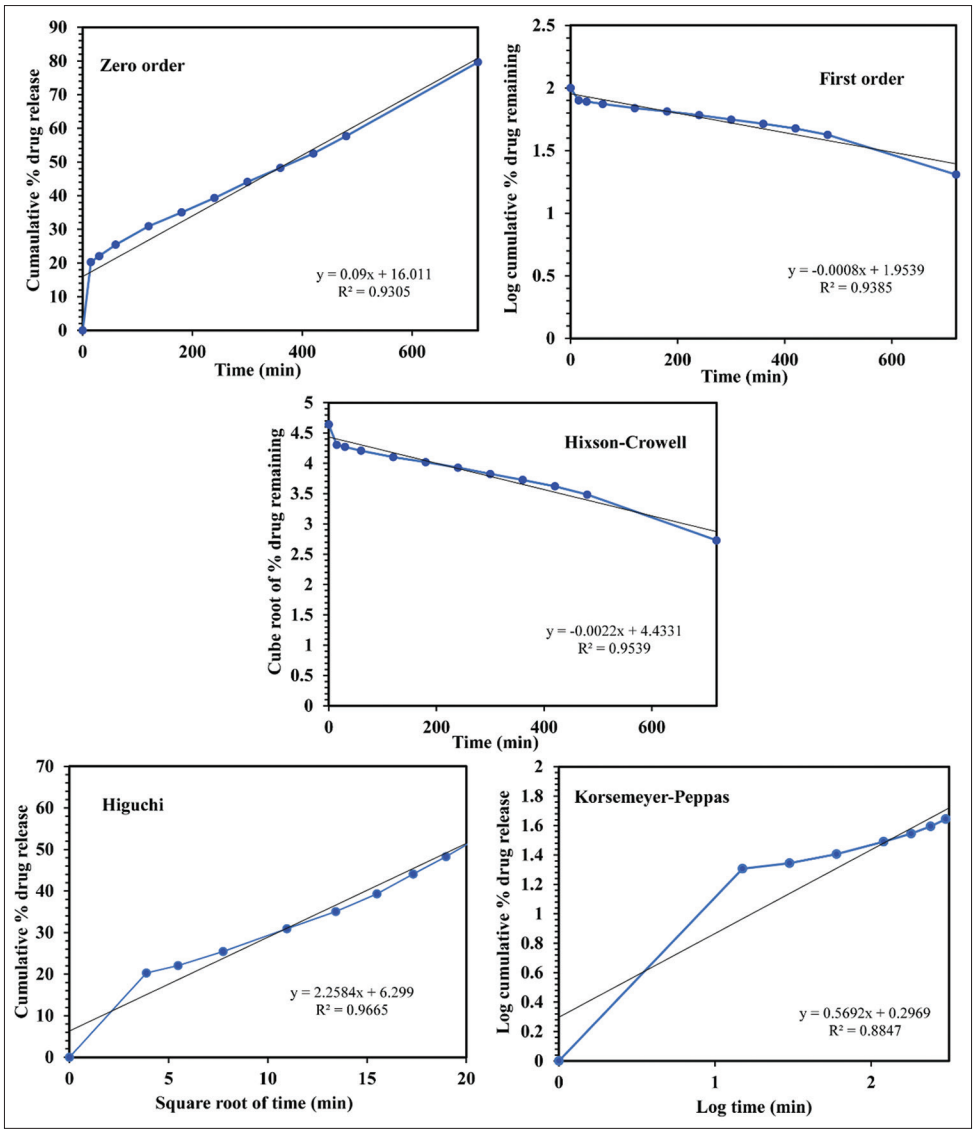

Fig. 19: Drug release kinetic plots of optimized formulation of FE-SLNs

Particle size, PDI and ZP analysis

The MPS plays vital role in stability, drug release, and cellular uptake of SLNs [53]. Studies suggested that smaller particle size enhances intestinal permeability through mechanisms such as endocytosis and lymphatic uptake and promotes a larger surface area for drug release. MPS of SLNs from 15 trial runs ranged between 384 nm and 928 nm, with the goal set to minimum. Following software analysis, the predicted MPS was 454.70 nm and the optimized batch yielded an actual size of 460.0 nm, which was near to software suggested value as shown in Table 4 and graphically represented in Fig. 17.

PDI describes how evenly or unevenly particles are distributed in sample [39]. It provides understanding about homogeneity of nanoparticle system. In general, in case of lipid based nanocarriers, the samples are said to be monodispersed when the PDI is ≤0.3 and PDI ≤0.1 indicates uniform distribution of particles [54] and PDI >0.3 indicates high PSD suggesting a wide spectrum of particle. PDI for fifteen trial runs observed from 0.147 to 0.855 and targeted to minimize. The PDI value of 0.205 was software suggested and 0.233 was exhibited by optimized SLN formulation, indicating a moderately monodisperse system. This value reflects a stable formulation for suitable oral delivery, with a narrow PSD that ensures drug release and absorption.

Zeta potential indicates the overall charge on the surface of particle. Higher (positive or negative) value experiences strong electrostatic repulsive forces, which reduces the particle aggregation [55]. A system having ±30 mv of surface charge or more is considered a stable formulation. ZP value for 15 trial runs was found in the range of −17.1–18.7 mV and marked maximum. Following software, the suggested Z-potential was 5.526 mV and −14.1 mV was experimentally calculated, as data recorded in Table 4.

% entrapment efficiency

Drug EE for the fifteen-trial runs was found in the range of 38.32–67.52% and marked maximum. 49.36% entrapment was predicted by software and the calculated value was 47.56% which was near to excepted figure of %EE as tabulated in Table 4.

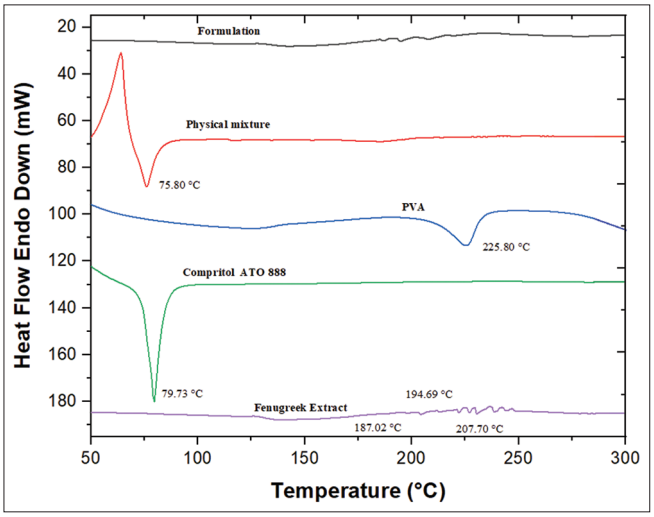

Fig. 20: DSC thermogram of drug, excipients, developed formulation and mixture of FE with excipients

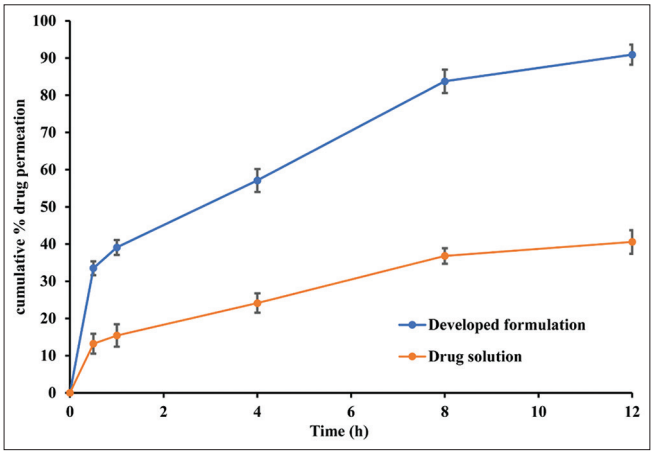

Fig. 21: Cumulative % drug permeation of developed fenugreek extract-solid lipid nanoparticles formulation and fenugreek extract solution (mean±SD, n=3)

In vitro drug release study

Drug release of formulations (SLN1-SLN15) was recorded as 8.9–19.7% at 0.5 h, 15.26–23.00% at 1 h, 30.92–48.44% at 4 h, 50.86–70.5% at 8 h and 65.78–88.5% at 12 h and target was to achieve highest. Post software analysis, suggested drug release was 17.63% at 0.5 h at 21.46% at 1 h, 41.63% 4 h, 64.8% at 8 h and 82.95% at 12 h. The calculated %CDR of the final batch was found to be 20.27% at 0.5 h, 22.06%, at 1h, 39.30% at 4 h, 57.52% at 8 h and, 79.66% at 12 h which was relatively near to the figure expected, the comparison data is summarized in Table 4. An overlay plot (Fig. 18a) and regression plot of software predicted vs. practically observed cumulative %drug release profile is depicted in Fig. 18b.

In vitro drug release kinetics

The release behavior was assessed using zero-order, first-order, Higuchi, Hixson-Crowell, and Korsmeyer-Peppas were studied and graphs were plotted as shown in Fig. 18. The Regression coefficient (R^2) values are tabulated in Table 6. Among these, Higuchi model showed the best fit based on its highest R^2 value (0.9665) indicating the release of drug from the FE-SLNs was governed primarily by utilizing diffusion process.

DSC

A DSC thermogram was used to analyze the nature of the FE and excipients, as well as their interactions. The thermograms were recorded for compritol 888 ATO, PVA, FE, lyophilized FE-SLNs and a physical mixture of drug with excipients as represented in Fig. 20. FE indicated a distinct endothermic peak at 187.02°C, 194.0°C, 207°C. PVA at 225.80°C, compritol 888 ATO at 79.73°C showed its crystalline nature. The lack of a distinct peak in the formulation confirms its amorphous state, suggesting successful drug encapsulation. In contrast, the physical mixture showed sharp endothermic peaks for the FE and excipients, indicating no chemical interactions. The thermogram results confirm that both the FE and excipients were pure and free from any foreign materials.

Ex vivo drug absorption study

Everted intestinal sac was employed to study how drug passes through intestine, helping to predict how it would behave in the body. Cylindrical sections of the intestine, each 6 cm long with an inner diameter of 0.60 cm were used, giving a surface area of 11.86 cm^2 for each piece [49]. The data of %drug permeated through the membrane from developed formulation and drug solution are tabulated in Table 5 and graphically depicted in Fig. 21.

The cumulative %drug permeation for the drug solution was 40.58% in comparison with the developed formulation showed much higher permeation of 90.90%. The apparent permeability coefficient and flux (Jss) was 6.30×10^{-3} cm/h and 3.50×10^{-3} ug/cm^2/s for FE-SLNs (developed formulation) and 2.91×10^{-3} cm/h and 1.61×10^{-3} ug/cm^2/s for drug solution, respectively. The small size of the SLNs likely made it easier for FE to pass through the membrane, further improving the permeation. The data suggest that FE was absorbed better in the GI tract when delivered through SLNs [25].

Table 6: Drug release kinetic data of optimized formulation

S. No.	Models	Equation	R^2	K
1.	Zero order	$Q_t=Q_{0+}k_0t$	0.9305	0.09
2.	First order	$LogQ=Log\ Q_0-kt/2.303$	0.9385	0.0008
3.	Higuchi	$Q_0-Q_t=kt^{1/2}$	0.9665	2.2584
4.	Hixson-Crowel	$Q_0^{1/3}-Qt^{1/3}=kt$	0.9539	0.0022
5.	Korsmeyer-Peppas	$Log\ (Q_0-Q_t)=logk+nlogt$	0.8847	0.5692

Q0=Initial amount, Qt=Drug amount remaining at time t, k=Rate constant, and t=Time

CONCLUSION

Development and optimization of FE-SLNs were successfully accomplished by BBD. Based on preliminary trials, lipid (compritol 888 ATO), emulsifier conc. (PVA), and homogenization speed (rpm) chosen as independent variables. Meanwhile, MPS, ZP, PDI, %EE, and %CDR at 0.5, 1, 4, 8, and 12 h were selected as dependent variables. The design expert software generated 15 optimization trial formulations. The experimental data from these batches were analyzed statistically, with the goal for minimum MPS, and PDI and maximum ZP, %EE, along with %CDR at the specified time points. Various solutions were suggested by the software and from those solutions, a batch having maximum desirability was finalized. The software suggested optimized formulation composition containing 400 mg lipid content, 0.303% surfactant conc. and 12610.6 rpm as homogenization speed. The developed FE-SLNs possessed all the desired physicochemical properties, CQAs in the acceptable range. Characterization results revealed MPS of 460.0 nm, ZP of −14.1 mV, PDI of 0.233, %EE of 47.56%, and %CDR values of 20.27%, 22.06%, 39.30%, 57.52%, and 79.66% at 0.5, 1, 4, 8, and 12 h, respectively. The outcomes of drug release showed that the developed SLNs formulation provides sustained drug release profile, fitting Higuchi's kinetic model. The *ex vivo* GI absorption study showed that the cumulative % drug permeation for drug solution was found to be 40.58% in comparison with the developed formulation showed much higher permeation, with 90.90%.The P_{app} coefficient for FE-SLNs (developed formulation) was found to 6.3×10^{-3} cm/h and 2.9×10^{-3} cm/h for drug solution which was more than two-fold higher in developed formulation in comparison to pure drug solution. According to all conclusions obtained from experimental work, it can be concluded that FE-loaded SLNs possess better pharmaceutical properties with enhanced permeation and absorption The developed SLNs were found to show promise for enhancing oral bioavailability based on *in vitro* and *ex vivo* results and that future *in vivo* studies are warranted to confirm the therapeutic potential.

ACKNOWLEDGMENT

The authors are grateful to Jamia Hamdard University, Delhi, for carrying out TEM analysis.

AUTHOR CONTRIBUTIONS

Dr. Prakash K. Soni: Conceptualized and supervised the whole research work.

Aditi Agrawal: Performed all the experiments, data observation, and manuscript writing.

Reena Soni: Contributed in material procurement, data analysis, and manuscript drafting.

Dr. Suresh K. Paswan: Technical inputs and machine handling, data checking.

FUNDING

There is no funding to report.

CONFLICT OF INTEREST

The authors report no financial or any other conflicts of interest in this work.

ETHICAL APPROVALS

This study does not associate with experiments on animals or human subjects.

REFERENCES

1. Dehariya P, Soni R, Paswan SK, Soni PK. Design of experiment based formulation optimization of chitosan-coated nano-liposomes of progesterone for effective oral delivery. J Appl Pharm Sci. 2023;13(06):256-70. doi: 10.7324/JAPS.2023.142351
2. Alqahtani MS, Kazi M, Alsenaidy MA, Ahmad MZ. Advances in oral drug delivery. Front Pharmacol. 2021;12:618411. doi: 10.3389/fphar.2021.618411, PMID 33679401
3. Ahadian S, Finbloom JA, Mofidfar M, Diltemiz SE, Nasrollahi F, Davoodi E, *et al.* Micro and nanoscale technologies in oral drug delivery. Adv Drug Deliv Rev. 2020;157:37-62. doi: 10.1016/j.addr.2020.07.012, PMID 32707147
4. Homayun B, Lin X, Choi HJ. Challenges and recent progress in oral drug delivery systems for biopharmaceuticals. Pharmaceutics. 2019;11(3):129. doi: 10.3390/pharmaceutics11030129, PMID 30893852
5. Opanasopit P, Aumklad P, Kowapradit J, Ngawhiranpat T, Apirakaramwong A, Rojanarata T, *et al.* Effect of salt forms and molecular weight of chitosans on *in vitro* permeability enhancement in intestinal epithelial cells (Caco-2). Pharm Dev Technol. 2007;12(5):447-55. doi: 10.1080/10837450701555901, PMID 17963144
6. Hua S. Advances in oral drug delivery for regional targeting in the gastrointestinal tract - influence of physiological, pathophysiological and pharmaceutical factors. Front Pharmacol. 2020;11:524. doi: 10.3389/fphar.2020.00524, PMID 32425781
7. Yadav UC, Baquer NZ. Pharmacological effects of *Trigonella foenum-graecum* L. in health and disease. Pharm Biol. 2014;52(2):243-54. doi: 10.3109/13880209.2013.826247, PMID 24102093
8. Sindhu RK, Goyal A, Algın Yapar EA, Cavalu S. Bioactive compounds and nanodelivery perspectives for treatment of cardiovascular diseases. Appl Sci. 2021;11(22):11031. doi: 10.3390/app112211031
9. Walia A, Gupta AK, Sharma V. Role of bioactive compounds in human health. Acta Sci Med Sci. 2019;3(9):25-33.
10. Gershenzon J, Dudareva N. The function of terpene natural products in the natural world. Nat Chem Biol. 2007;3(7):408-14. doi: 10.1038/nchembio.2007.5, PMID 17576428
11. Dar RA, Shahnawaz M, Ahanger MA, Majid I. Exploring the diverse bioactive compounds from medicinal plants: A review. J Phytopharmacol. 2023;12(3):189-95. doi: 10.31254/phyto.2023.12307
12. Block E. The chemistry of garlic and onions. Sci Am. 1985;252(3):114-9. doi: 10.1038/scientificamerican0385-114, PMID 3975593
13. Calder PC. Polyunsaturated fatty acids and inflammation. Prostaglandins Leukot Essent Fatty Acids. 2006;75(3):197-202. doi: 10.1016/j.plefa.2006.05.012, PMID 16828270
14. Lv Y, Li W, Liao W, Jiang H, Liu Y, Cao J, *et al.* Nano-drug delivery systems based on natural products. Int J Nanomedicine. 2024;19:541-69. doi: 10.2147/IJN.S443692, PMID 38260243
15. Kumari S, Goyal A, Sönmez Gürer E, Algın Yapar E, Garg M, Sood M, *et al*. Bioactive loaded novel nano-formulations for targeted drug delivery and their therapeutic potential. Pharmaceutics. 2022;14(5):1091. doi: 10.3390/pharmaceutics14051091, PMID 35631677
16. Sarwar S, Hanif MA, Ayub MA, Boakye YD, Agyare C. Fenugreek. In: Medicinal Plants of South Asian. Netherlands: Elsevier; 2020. p. 257-71. doi: 10.1016/B978-0-08-102659-5.00020-3
17. Jhajhria A, Kumar K. Fenugreek with its medicinal applications. Int J Pharm Sci Rev Res. 2016;41(1):194-201.
18. Yao D, Zhang B, Zhu J, Zhang Q, Hu Y, Wang S, *et al*. Advances on application of fenugreek seeds as functional foods: Pharmacology, clinical application, products, patents and market. Crit Rev Food Sci Nutr. 2020;60(14):2342-52. doi: 10.1080/10408398.2019.1635567, PMID 31286789
19. Tewari A, Singh R, Brar JK. Pharmacological and therapeutic properties of fenugreek (*Trigonella foenum-graecum*) seed: A review. J Phytopharmacol. 2024;13(2):97-104. doi: 10.31254/phyto.2024.13203
20. Majumder J, Taratula O, Minko T. Nanocarrier-based systems for targeted and site specific therapeutic delivery. Adv Drug Deliv Rev. 2019;144:57-77. doi: 10.1016/j.addr.2019.07.010, PMID 31400350
21. Lin CH, Chen CH, Lin ZC, Fang JY. Recent advances in oral delivery of drugs and bioactive natural products using solid lipid nanoparticles as the carriers. J Food Drug Anal. 2017;25(2):219-34. doi: 10.1016/j.jfda.2017.02.001, PMID 28911663.
22. Pathak K, Raghuvanshi S. Oral bioavailability: Issues and solutions via nanoformulations. Clin Pharmacokinet. 2015;54(4):325-57. doi: 10.1007/s40262-015-0242-x, PMID 25666353
23. Reinholz J, Landfester K, Mailänder V. The challenges of oral drug delivery via nanocarriers. Drug Deliv. 2018;25(1):1694-705. doi: 10.1080/10717544.2018.1501119, PMID 30394120
24. Sadeghi S, Lee WK, Kong SN, Shetty A, Drum CL. Oral administration of protein nanoparticles: An emerging route to disease treatment. Pharmacol Res. 2020;158:104685. doi: 10.1016/j.phrs.2020.104685,

PMID 32097749
25. Paliwal R, Paliwal SR, Kenwat R, Kurmi BD, Sahu MK. Solid lipid nanoparticles: A review on recent perspectives and patents. Expert Opin Ther Pat. 2020;30(3):179-94. doi: 10.1080/13543776.2020.1720649, PMID 32003260
26. Kathe N, Henriksen B, Chauhan H. Physicochemical characterization techniques for solid lipid nanoparticles: Principles and limitations. Drug Dev Ind Pharm. 2014;40(12):1565-75. doi: 10.3109/03639045.2014.909840, PMID 24766553
27. Akbari J, Saeedi M, Ahmadi F, Hashemi SM, Babaei A, Yaddollahi S, *et al*. Solid lipid nanoparticles and nanostructured lipid carriers: A review of the methods of manufacture and routes of administration. Pharm Dev Technol. 2022;27(5):525-44. doi: 10.1080/10837450.2022.2084554, PMID 35635506
28. Mirchandani Y, Patravale VB, Brijesh S. Solid lipid nanoparticles for hydrophilic drugs. J Control Release. 2021;335:457-64. doi: 10.1016/j.jconrel.2021.05.032, PMID 34048841
29. Harde H, Das M, Jain S. Solid lipid nanoparticles: An oral bioavailability enhancer vehicle. Expert Opin Drug Deliv. 2011;8(11):1407-24. doi: 10.1517/17425247.2011.604311, PMID 21831007
30. Ganesan P, Narayanasamy D. Lipid nanoparticles: Different preparation techniques, characterization, hurdles, and strategies for the production of solid lipid nanoparticles and nanostructured lipid carriers for oral drug delivery. Sustain Chem Pharm. 2017;6:37-56. doi: 10.1016/j.scp.2017.07.002
31. Viegas C, Patrício AB, Prata JM, Nadhman A, Chintamaneni PK, Fonte P. Solid lipid nanoparticles vs. nanostructured lipid carriers: A comparative review. Pharmaceutics. 2023;15(6):1593. doi: 10.3390/pharmaceutics15061593, PMID 37376042
32. Mishra V, Bansal KK, Verma A, Yadav N, Thakur S, Sudhakar K, *et al*. Solid lipid nanoparticles: Emerging colloidal Nano drug delivery systems. Pharmaceutics. 2018;10(4):191. doi: 10.3390/pharmaceutics10040191, PMID 30340327
33. Salah E, Abouelfetouh MM, Pan Y, Chen D, Xie S. Solid lipid nanoparticles for enhanced oral absorption: A review. Colloids Surf B Biointerfaces. 2020;196:111305. doi: 10.1016/j.colsurfb.2020.111305, PMID 32795844
34. Mukherjee S, Ray S, Thakur RS. Solid lipid nanoparticles: A modern formulation approach in drug delivery system. Indian J Pharm Sci. 2009;71(4):349-58. doi: 10.4103/0250-474X.57282, PMID 20502539
35. Rahman Z, Zidan AS, Khan MA. Non-destructive methods of characterization of risperidone solid lipid nanoparticles. Eur J Pharm Biopharm. 2010;76(1):127-37. doi: 10.1016/j.ejpb.2010.05.003, PMID 20470882
36. Chandwani S, Saini TR, Soni R, Paswan SK, Soni PK. Box-Behnken design optimization of salicylic acid loaded liposomal gel formulation for treatment of foot corn. Int J Appl Pharm. 2023;15(3):220-33. doi: 10.22159/ijap.2023v15i3.47455
37. Prakash A, Soni PK, Paswan SK, Saini TR. Formulation and optimization of mucoadhesive buccal film for nicotine replacement therapy. Int J Appl Pharm. 2023;15(3):100-12. doi: 10.22159/ijap.2023v15i3.47412
38. Soni PK, Saini TR. Non-ionic surfactant vesicles (niosomes) based novel ophthalmic formulation of timolol maleate. J Drug Deliv Ther. 2017;7(7):59-61. doi: 10.22270/jddt.v7i7.1587
39. Soni PK, Saini TR. Purification of drug loaded liposomal formulations by a novel stirred cell ultrafiltration technique. Pharm Nanotechnol. 2021;9(5):347-60. doi: 10.2174/2211738509666211124145848, PMID 34819014
40. Soni PK, Saini TR. Development and evaluation of HP-β-CD complexation based novel ophthalmic gel formulation of nepafenac. Int J Pharm Sci Res. 2019;10(12):5707-14. doi: 10.13040/IJPSR.0975-8232.10(12).5707-14
41. Pandita D, Kumar S, Poonia N, Lather V. Solid lipid nanoparticles enhance oral bioavailability of resveratrol, a natural polyphenol. Food Res Int. 2014;62:1165-74. doi: 10.1016/j.foodres.2014.05.059
42. Jain P, Soni R, Paswan SK, Soni PK. Ketoconazole laden microemulsion based gel formulation against skin fungal infection. Int J Appl Pharm. 2023;15(3):49-60. doi: 10.22159/ijap.2023v15i3.47456
43. Available from: https://www.himedialabs.com/in/la395-dialysis-membrane-110.html [Last accessed on 2025 Jan 08].
44. Paswan SK, Saini TR. Comparative evaluation of *in vitro* drug release methods employed for nanoparticle drug release studies. Diss Technol. 2021;28(4):30-8. doi: 10.14227/DT280421P30
45. Soni PK, Saini TR. Formulation design and optimization of cationic-charged liposomes of brimonidine tartrate for effective ocular drug delivery by design of experiment (DoE) approach. Drug Dev Ind Pharm. 2021;47(11):1847-66. doi: 10.1080/03639045.2022.2070198, PMID 35484943
46. Chaturvedi P, Soni PK, Paswan SK. Designing and development of gastroretentive mucoadhesive microspheres of cefixime trihydrate using spray dryer. Int J Appl Pharm. 2023;15(2):185-93. doi: 10.22159/ijap.2023v15i2.45399
47. Paswan SK. Designing and characterization of polymeric microparticles containing agomelatine-loaded mesoporous silica nanoparticles for a controlled drug delivery system. Asian J Pharm. 2023;17(3):400-11. doi: 10.22377/ajp.v17i03.4982
48. Gamboa JM, Leong KW. *In vitro* and *in vivo* models for the study of oral delivery of nanoparticles. Adv Drug Deliv Rev. 2013;65(6):800-10. doi: 10.1016/j.addr.2013.01.003, PMID 23415952
49. Foudah AI, Ayman Salkini M, Alqarni MH, Alam A. Preparation and evaluation of antidiabetic activity of mangiferin-loaded solid lipid nanoparticles. Saudi J Biol Sci. 2024;31(4):103946. doi: 10.1016/j.sjbs.2024.103946, PMID 38384280
50. Jafari SM, Assadpoor E, He Y, Bhandari B. Re-coalescence of emulsion droplets during high-energy emulsification. Food Hydrocoll. 2008;22(7):1191-202. doi: 10.1016/j.foodhyd.2007.09.006
51. Anton N, Benoit JP, Saulnier P. Design and production of nanoparticles formulated from nano-emulsion templates-a review. J Control Release. 2008;128(3):185-99. doi: 10.1016/j.jconrel.2008.02.007, PMID 18374443
52. Müller RH, Mäder K, Gohla S. Solid lipid nanoparticles (SLN) for controlled drug delivery - a review of the state of the art. Eur J Pharm Biopharm. 2000;50(1):161-77. doi: 10.1016/s0939-6411(00)00087-4, PMID 10840199
53. Rao H, Ahmad S, Madni A, Rao I, Ghazwani M, Hani U, *et al*. Compritol-based alprazolam solid lipid nanoparticles for sustained release of alprazolam: Preparation by hot melt encapsulation. Molecules. 2022;27(24):8894. doi: 10.3390/molecules27248894, PMID 36558027
54. Hassan H, Bello RO, Adam SK, Alias E, Meor Mohd Affandi MM, Shamsuddin AF, *et al.* Acyclovir-loaded solid lipid nanoparticles: Optimization, characterization and evaluation of its pharmacokinetic profile. Nanomaterials (Basel). 2020;10(9):1785. doi: 10.3390/nano10091785, PMID 32916823
55. Das S, Chaudhury A. Recent advances in lipid nanoparticle formulations with solid matrix for oral drug delivery. AAPS PharmSciTech. 2011;12(1):62-76. doi: 10.1208/s12249-010-9563-0, PMID 21174180